The Succession of Heat and Mass Driven Natural Convection Regimes Along a Vertical Impermeable Wall

Maria Neagu

Manufacturing Engineering Department,
"Dunarea de Jos" University of Galati

Abstract

This paper presents the analysis of the natural convection process that takes place near a vertical plane wall embedded in a constant temperature and linearly mass stratified fluid (the Prandtl number and the Smith number are smaller than 1.0, while the Lewis number is greater than 1.0). The wall has a constant temperature, while the flux of a certain constituent is constant at this boundary. The scale analysis and the finite differences method are used as techniques of work. The scale analysis proves the existence, at equilibrium, of heat and/or mass driven convection regimes along the wall. The finite differences method is used solve the governing equations and to verify the scale analysis results using two particular parameters sets.

Keywords: natural convection, constant mass flux, scale analysis, finite differences method

1. Introduction

The analysis of the natural convection process along a vertical plane wall is a classical problem that was taken into consideration along the past decades in applications of a specific or general character (Armfield, Patterson & Lin, 2007; Lin, Armfield & Patterson, 2008; Mongruel, Cloitre and Allain, 1996; Neagu, 2018, 2021; Patterson, Lei, Armfield & Lin, 2009; Saha, Patterson and Lei, 2010; Saha, Brown & Gu, 2012).

This research analysis refers to a vertical plane wall that have a constant temperature and that registers a constant flux of a certain constituent at it. The environment is air ($\mathrm{Pr}=0.72$ in this paper) while the Lewis number is greater than 1.0 ($\mathrm{Le}\geq 1$) and the Smith number is smaller than 1.0 ($\mathrm{Sch}<1$). The environment is mass stratified, while its temperature is constant.

The scale analysis is performed and the results are verified by solving the governing equations using the finite differences method for two particular parameters sets: $Ra = 5000$, $N = 1$, $Le = 1$, $Pr = 0{,}72$, $S_C = 0.08$ and $Ra = 5000$, $N = 5$, $Le = 2$, $Pr = 0{,}72$, $S_C = 0.04$.

2. Mathematical Formulation

Figure 1 presents the vertical plane wall and the x-y system of co-ordinates associated to it in dimensional (Fig. 1a) and in dimensionless (Fig. 1b) representations.

The temperature at the wall is T_w, while the environment has a constant temperature, T_∞. The mass flux of a certain constituent, m_w, is constant at the wall, while the environment registers a concentration of the constituent of $C_{\infty,x} = C_{\infty,0} + s_C \cdot x$.

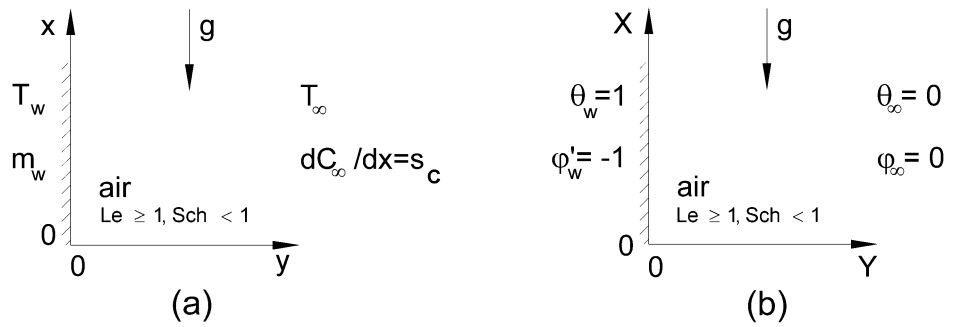

Fig. 1. (a) The dimensional problem; (b) the dimensionless problem.

2018):

$$\frac{\partial v}{\partial x} + \frac{\partial u}{\partial y} = 0; \tag{1}$$

$$\frac{\partial u}{\partial t} + u \cdot \frac{\partial u}{\partial y} + v \cdot \frac{\partial u}{\partial x} = -\frac{\partial p}{\partial y} + \nu\left(\frac{\partial^2 u}{\partial x^2} + \frac{\partial^2 u}{\partial y^2}\right); \tag{2}$$

$$\frac{\partial v}{\partial t} + u \cdot \frac{\partial v}{\partial y} + v \cdot \frac{\partial v}{\partial x} = -\frac{\partial p}{\partial x} + \nu\left(\frac{\partial^2 v}{\partial x^2} + \frac{\partial^2 v}{\partial y^2}\right) + g\beta_t T + g\beta_c C; \tag{3}$$

$$\frac{\partial T}{\partial t}+u\cdot\frac{\partial T}{\partial y}+v\cdot\frac{\partial T}{\partial x}=\alpha\left(\frac{\partial^2 T}{\partial x^2}+\frac{\partial^2 T}{\partial y^2}\right); \tag{4}$$

$$\frac{\partial C}{\partial t}+u\cdot\frac{\partial C}{\partial y}+v\cdot\frac{\partial C}{\partial x}+v\cdot s_c=D\left(\frac{\partial^2 C}{\partial x^2}+\frac{\partial^2 C}{\partial y^2}\right), \tag{5}$$

and the boundary conditions (Neagu, 2018):

$$u=v=0,\ T=T_w,\ \frac{\partial C}{\partial y}=-\Gamma_w \text{ at } y=0; \tag{6}$$

$$v=0,\ T=T_\infty,\ C=C_{\infty,x} \text{ as } y\to\infty; \tag{7}$$

$$v=0,\ T=T_\infty,\ C=C_{\infty,0} \text{ at } x=0; \tag{8}$$

$$\frac{\partial^2 u}{\partial x^2}=\frac{\partial^2 v}{\partial x^2}=\frac{\partial^2 T}{\partial x^2}=\frac{\partial^2 C}{\partial x^2}=0 \text{ at } x=h, \tag{9}$$

define the point of start of the scale analysis.

3. Scale Analysis

This analysis follows the same pattern used before in the scientific literature (Bejan 1995; Neagu, 2018, 2021) for a better correlation, comprehension of the research characteristics and following the evolution of the natural convection regime that develops along the boundary: the initial state (section 3.1), the heat driven convection (HDC) regime (section 3.2) and the mass driven convection (MDC) regime (section 3.3).

3.1. The Initial State

Because this section is similar to the results of previous analysis, only the most significant results will be mentioned here (Neagu, 2018):

the boundary layer thickness of the temperature field:

$$\delta_T\sim\alpha^{1/2}\cdot t^{1/2}; \tag{10}$$

the boundary layer thickness of the concentration field:

$$\delta_C\sim D^{1/2}\cdot t^{1/2}; \tag{11}$$

the heat driven convection regimes that exists at the beginning at each point along the wall will be replaced by a mass driven convection regime only if the equilibrium time of the regime is bigger than the transition time, t_{trz}:

$$t_{trz} \sim L^2 \cdot \left(N^2 D\right)^{-1}; \tag{12}$$

the inequality $s_C > \partial C / \partial x$, that is valid at the beginning at each point of the wall, ceases to be valid if the equilibrium time of the regime is bigger than t_s:

$$t_s \sim \frac{s_C{}^2 x^2}{\Gamma_w{}^2 D}. \tag{13}$$

3.2. The Heat Driven Convection Regime

If $Pr < 1$ and $Le \geq 1$, Saha, Patterson and Lei (2010) prove that the order of magnitude of the vertical velocity is:

$$v_T \sim \frac{g\beta_t t}{1+Pr}\Delta T. \tag{14}$$

Invoking the equilibrium between the horizontal diffusion and the vertical convection of heat, the temperature equilibrium time, boundary layer thickness and vertical velocity orders of magnitude are (Neagu, 2018):

$$\left(t_{ech,T}\right)_T \sim \frac{L^2}{\alpha}\left[\frac{X(1+Pr)}{Ra \cdot Pr}\right]^{1/2}; \tag{15}$$

$$\left(\delta_{ech,T}\right)_T \sim L \cdot \left[\frac{X(1+Pr)}{Ra \cdot Pr}\right]^{1/4}; \tag{16}$$

$$V_T \sim \left(\frac{X \cdot Ra \cdot Pr}{1+Pr}\right)^{1/2}. \tag{17}$$

a. Scale analysis of the concentration field in the HDC regime

b. In this case, the velocity order of magnitude for the concentration field is v_T.

c. Two situations appear:

d. if in the left side of equation (5) $v \cdot \partial C / \partial x \geq v \cdot s_C$, then the equilibrium between the horizontal diffusion of the constituent and the vertical convection of it gives us the equilibrium time of the concentration field:

$$\left(t_{ech,C}\right)_T \sim \frac{L^2}{D}\left[\frac{X\,Pr(1+Pr)}{Sch^2\cdot Ra}\right]^{1/2}. \quad (18)$$

Further, using equation (11), the boundary layer thickness order of magnitude becomes:

$$\left(\delta_{ech,C}\right)_T \sim L\left[\frac{X\,Pr(1+Pr)}{Sch^2\cdot Ra}\right]^{1/4}. \quad (19)$$

The equilibrium time of the concentration field, $\left(t_{ech,C}\right)_T$, is bigger than the transition time, t_{trz}, if:

$$X > X_{trz,C} = \frac{Sch^2}{N^4}\frac{Ra}{Pr(1+Pr)} \quad (20)$$

b. if, in equation (5), $v\cdot\partial C/\partial x < v\cdot s_C$, then the concentration equilibrium time and boundary layer thickness are:

$$\left(t_{ech,Sc}\right)_T \sim \frac{L^2}{D}\frac{Pr(1+Pr)}{S_C^2\cdot Sch^2\cdot Ra\cdot X}; \quad (21)$$

$$\left(\delta_{ech,Sc}\right)_T \sim L\left[\frac{Pr(1+Pr)}{Ra\cdot X\cdot S_C^2\cdot Sch^2}\right]^{1/2}. \quad (22)$$

The equilibrium time $\left(t_{ech,,Sc}\right)_T$ is compared to t_{trz} and t_s:

b1) the equilibrium time $\left(t_{ech,,Sc}\right)_T$ is bigger than the transition time, t_{trz}, if:

$$X > X_{trz,Sc} = \frac{N^2\,Pr(1+Pr)}{Sc^2 Sch^2 Ra}; \quad (23)$$

b2) the inequality $\left(t_{ech,Sc}\right)_T < t_s$ is restricted to the following domain:

$$X \geq X_{S,T} = \left[\frac{Pr(1+Pr)}{S_c^4\cdot Sch^2\cdot Ra}\right]^{1/3}. \quad (24)$$

1. The analysis of the results presented above reveals that there are only two possibilities:
2. a HDC regime along the wall if $X_{trz,Sc} < X_{S,T} < X_{trz,C}$ (figure 2 (a)) or

$$\frac{Ra\cdot S_C\cdot Sch^2}{Pr(1+Pr)\cdot N^3} \geq 1 \quad (25)$$

a HDC regime in the $\left[0, X_{trz,C}\right]$ domain and a MDC regime in the $\left[X_{trz,C}, \infty\right)$ domain (see figure 2 (b)) if $Ra \cdot S_C \cdot Sch^2 / \left[N^3 Pr(1+Pr)\right] < 1$.

3.3. The Mass Driven Convection Regime

The vertical velocity order of magnitude was derived by Lin, Armfield and Patterson (2008):

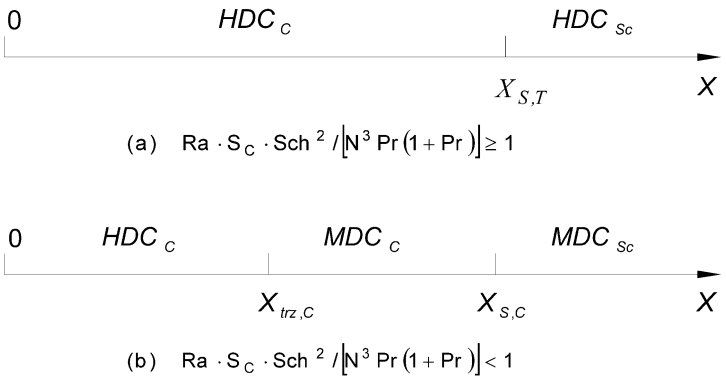

Fig. 2. The heat and mass driven natural convection regimes sequence. (a) $Ra \cdot S_C \cdot Sch^2 / \left[N^3 Pr(1+Pr)\right] \geq 1$; (b) $Ra \cdot S_C \cdot Sch^2 / \left[N^3 Pr(1+Pr)\right] < 1$.

$$v = g\beta_C \Gamma_w D^{1/2} t^{3/2} \left(1 - \sqrt{Sch}\right). \tag{26}$$

3.3.1. MDC_{Sc} Regime.

In this case, the equilibrium between the horizontal diffusion and the vertical convection of the constituent requires: $v \cdot s_c \sim D\left(\frac{\partial^2 C}{\partial y^2}\right)$ or $v \cdot s_c \sim D\frac{\Gamma_w}{D^{1/2} t^{1/2}}$. Replacing v from equation (26), the concentration equilibrium time and the boundary layer thickness are:

$$\left(t_{ech,Sc}\right)_c \sim L^2 / D / \left[Ra \cdot N \cdot S_C \cdot Le \cdot Sch\left(1 - \sqrt{Sch}\right)\right]^{1/2}; \tag{27}$$

$$\left(\delta_{ech,Sc}\right)_c \sim L / \left[Ra \cdot N \cdot S_C \cdot Le \cdot Sch\left(1 - \sqrt{Sch}\right)\right]^{1/4}. \tag{28}$$

At equilibrium, the vertical velocity order of magnitude scales as:

$$V_{Sc} \sim \left[Ra \cdot N \cdot Sch \cdot \left(1 - \sqrt{Sch}\right) / (Le \cdot Sch)^3\right]^{1/4}. \tag{29}$$

The inequality $\left(t_{ech,Sc}\right)_C < t_s$ or

$$X > X_{S,C} = 1/\left[Ra \cdot N \cdot {S_C}^5 \cdot Le \cdot Sch \cdot \left(1-\sqrt{Sch}\right)\right]^{1/4} \quad (30)$$

defines the X co-ordinate that separates the MDC_C and the MDC_{Sc} regimes in the figure 2(b).

Scale analysis of the temperature field in the MDC_{Sc} regime. The equilibrium state requires:

$\left(v_C \frac{\delta_v}{\delta_T}\right) \cdot \frac{\partial T}{\partial x} \sim \alpha \cdot \frac{\partial^2 T}{\partial y^2}$ or $\left(v_C \frac{\sqrt{Sch} \cdot \delta_c}{\delta_T}\right) \cdot \frac{\Delta T}{x} \sim \alpha \frac{\Delta T}{\delta_T^2}$. Using the equation (10) and the equation (29), the equilibrium temperature boundary layer thickness order of magnitude is:

$$\left(\delta_{ech,T}\right)_{Sc} \sim L \cdot \left(Le \cdot X \cdot S_C\right). \quad (31)$$

3.3.2. MDC_C Regime

The equilibrium between the horizontal diffusion and the vertical convection requires $v_C \cdot \frac{\partial C}{\partial x} \sim D\left(\frac{\partial^2 C}{\partial y^2}\right)$ or $v_C \cdot \frac{1}{x} \sim D\frac{1}{\delta_C^2}$. Replacing the equations (11) and (29), the equilibrium time and the concentration boundary layer thickness become:

$$\left(t_{ech,C}\right)_C \sim L^2/D/\left[Ra \cdot N \cdot Le \cdot Sch\left(1-\sqrt{Sch}\right)\right]^{2/5}; \quad (32)$$

$$\left(\delta_{ech,C}\right)_C \sim L/\left[Ra \cdot N \cdot Le \cdot Sch\left(1-\sqrt{Sch}\right)\right]^{1/5}, \quad (33)$$

while the vertical velocity scales as:

$$V_C \sim \left[Ra \cdot N \cdot Sch \cdot \left(1-\sqrt{Sch}\right)\right]^{2/5} (X/Le)^{3/5}. \quad (34)$$

Scale analysis of the temperature field in the MDC_C regime.

The equilibrium between the thermal horizontal diffusion and the vertical thermal convection requires $v_C\left(\frac{\delta_V}{\delta_T}\right) \cdot \frac{\partial T}{\partial x} \sim \alpha\left(\frac{\partial^2 T}{\partial y^2}\right)$ or $v_C \frac{\sqrt{Sch} \cdot \delta_C}{\delta_T} \cdot \frac{\Delta T}{x} \sim \alpha \frac{\Delta T}{\delta_T^2}$. The temperature boundary layer thickness scales as:

$$\left(\delta_{ech,T}\right)_C \sim L\left[\frac{X \cdot Le^4}{Ra \cdot N \cdot Sch\left(1-\sqrt{Sch}\right)}\right]^{1/5}. \quad (35)$$

The validity of the scale analysis requires the following set of conditions:

if $Ra \cdot S_C \cdot Sch^2 / \left[N^3 Pr(1+Pr)\right] \geq 1$, the imposed conditions: $(\delta_{ech,T})_T << x$, $(\delta_{ech,C})_T << x$ and $(\delta_{ech,Sc})_T << x$ at $X = X_{S,T}$, leads us to the inequality: $S_C << \sqrt{Pr}$.

if $Ra \cdot S_C \cdot Sch^2 / \left[N^3 Pr(1+Pr)\right] < 1$, then the requirements: $(\delta_{ech,T})_T << x$ for $X = X_{trz,C}$; $(\delta_{ech,C})_C << x$, $(\delta_{ech,T})_C << x$, $(\delta_{ech,Sc})_C << x$ and $(\delta_{ech,T})_{Sc} << x$ for $X = X_{S,C}$ lead us to the requirement: $S_C << 1/Le$.

Further, the scale analysis results of section 3 will be verified using the finite differences method for two particular parameters sets.

4. Numerical Modeling

The stream function formulation of the velocity field, $U = -\partial\Psi/\partial X$, $V = \partial\Psi/\partial Y$, and the vorticity definition, $\zeta = \partial V/\partial Y - \partial U/\partial X$, define the dimensionless form of the governing equations

$$\zeta = \left(\frac{\partial^2\Psi}{\partial Y^2} + \frac{\partial^2\Psi}{\partial X^2}\right); \tag{36}$$

$$\frac{\partial\zeta}{\partial\tau} + U\frac{\partial\zeta}{\partial Y} + V\frac{\partial\zeta}{\partial X} = Pr\cdot\left(\frac{\partial^2\zeta}{\partial Y^2} + \frac{\partial^2\zeta}{\partial X^2}\right) + Ra\cdot Pr\cdot\left(\frac{\partial\theta}{\partial Y} + N\frac{\partial\varphi}{\partial Y}\right); \tag{37}$$

$$\frac{\partial\theta}{\partial\tau} + U\frac{\partial\theta}{\partial Y} + V\frac{\partial\theta}{\partial X} = \frac{\partial^2\theta}{\partial Y^2} + \frac{\partial^2\theta}{\partial X^2}; \tag{38}$$

$$\frac{\partial\varphi}{\partial\tau} + U\frac{\partial\varphi}{\partial Y} + V\frac{\partial\varphi}{\partial X} + VS_C = \frac{1}{Le}\left(\frac{\partial^2\varphi}{\partial Y^2} + \frac{\partial^2\varphi}{\partial X^2}\right). \tag{39}$$

The boundary conditions take the following form:

$$\Psi = \frac{\partial\Psi}{\partial Y} = 0,\ \frac{\partial\varphi}{\partial Y} = -1,\ \theta = 1 \text{ at } Y = 0; \tag{40}$$

$$\frac{\partial\Psi}{\partial Y} = 0,\ \zeta = 0,\ \theta = \varphi = 0 \text{ as } Y = L; \tag{41}$$

$$\Psi = 0,\ \zeta = 0,\ \theta = \varphi = 0 \text{ at } X = 0; \tag{42}$$

$$\frac{\partial^2\psi}{\partial X^2} = \frac{\partial^3\psi}{\partial X^3} = \frac{\partial^2\theta}{\partial X^2} = \frac{\partial^2\varphi}{\partial X^2} = 0 \text{ at } X = H. \tag{43}$$

The conservation equations (36)–(39) with the boundary conditions (40)–(43) were solved using the finite differences method. A software was built by Neagu (2018)

using a higher order hybrid scheme (Tennehill, Anderson & Pletcher, 1997) through an iterative process: at each time step, equation (36) was solved iteratively till the relative error of Ψ, at each point of the grid, became less than 10^{-6}. The iterative process stopped when the relative errors of θ, φ and ζ became less than 10^{-6} at each grid point.

5. Results and Discussions

Two particular parameter sets are used to run the program explained above:

The $Ra = 5000, N = 1, Le = 1, Pr = 0{,}72, S_C = 0.08$ parameters set is the example chosen to exemplify the $Ra \cdot S_C \cdot Sch^2 / \left[Pr(1+Pr) \cdot N^3\right] \geq 1$ case. The results of section 2 of this analysis tell us that a HDC (heat driven convection) regime is present, at equilibrium, along the vertical wall. Equation (24) indicates that the HDC_C $(\partial C / \partial X \geq S_C)$ and the HDC_{Sc} $(\partial C / \partial X < S_C)$ regimes are separated at the $X_{S,T} = 2.32$ abscissas. A computational dimensionless domain of 0.6×6.0 was discretised uniformly using a 61×301 grid for a sufficient accuracy.

The results for this particular parameters set are present by Fig. 3. It shows the temperature (Figure 3(a)), concentration (Figure 3(b)), stream function (Figure 3(c)) and $\partial C / \partial X$ (Figure 3(d)) fields. The concentration field (Figure 3(b)) is not greater than $1/N = 1.0$ and this is an indication that HDC regime is encountered along the entire wall. The $\partial C / \partial X$ field of Fig. 3(d) exceed 0.0 ($\partial c / \partial x > s_c$) if $X \geq 1.8$ a value close to the $X_{S,T}$ value indicated by equation (24).

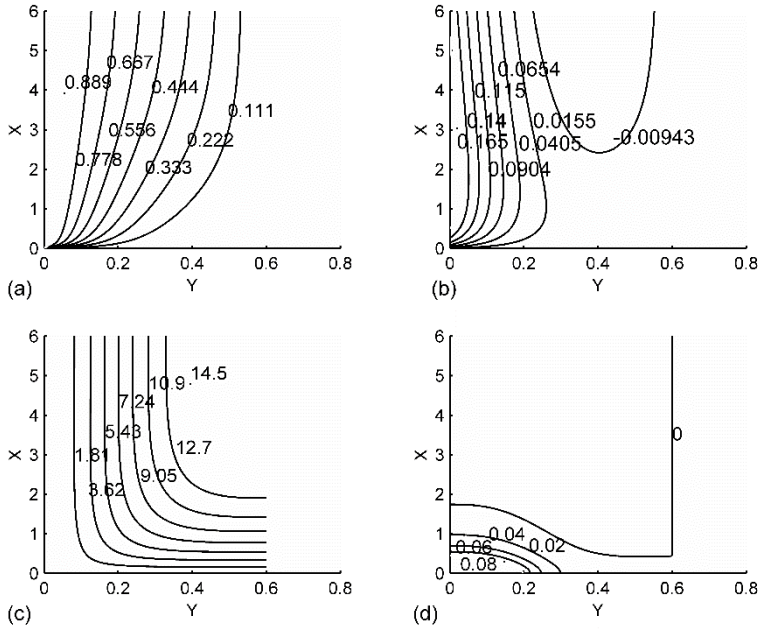

Fig. 3. The dimensionless temperature (a), concentration (b), stream function (c) and $\partial\varphi/\partial x$ (d) fields for $Ra=5000$, $N=1$, $Le=1$, $Pr=0.72$ and $S_C=0.08$.

In the HDC_C region, three sections present the temperature (Figure 4(a)), the concentration (Figure 4(b)) and the vertical velocity (Figure 4(c)) plots for thre abscissa: 0.5; 1.0 and 1.5. The scaled plots (Fig. 4(d)-Fig. 4(f)), realised using the equations (16), (17) and (19), collapse indicating the validity of the scale analysis.

Similarly, in the HDC_{Sc} region three abscissa: 3, 4 and 5, are chosen and their temperature (Figure 5(a)), concentration (Figure 5(b)) and vertical velocity (Figure 5(c)) plots are presented. Their scaled plots: (Figure 5(d), Figure 5(e) and Figure 5(f)), are realised using the equations (16), (17) and (22). The figures 3, 4 and 5 prove the validity of the scale analysis for the $Ra\cdot S_C\cdot Sch^2/\left[Pr(1+Pr)\cdot N^3\right]\geq 1$ case.

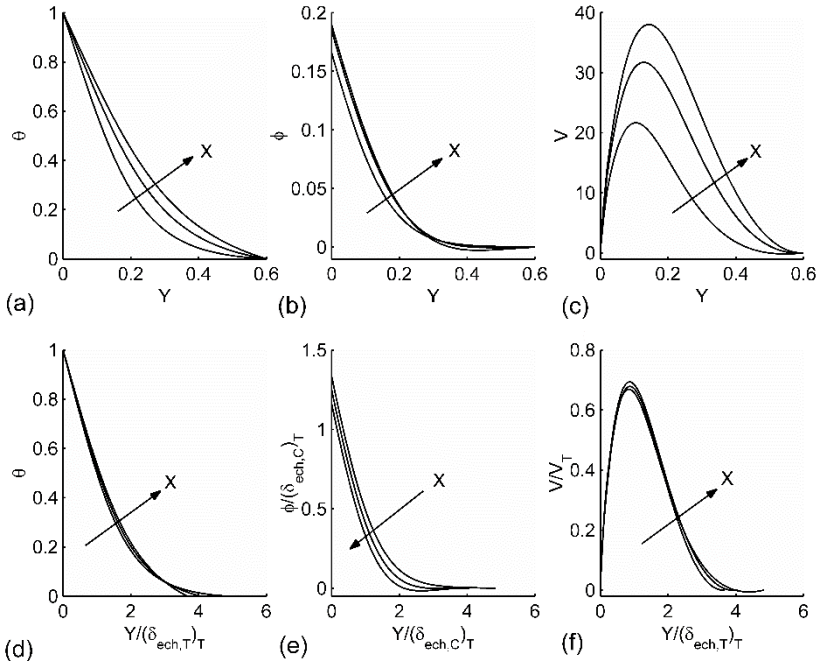

Fig. 4. The (a) θ, (b) φ and (c) V variations as a function of Y and the scaled (d) temperature, (e) concentration and (f) vertical velocity plots for the abscissa: 0.5, 1.0 and 1.5.

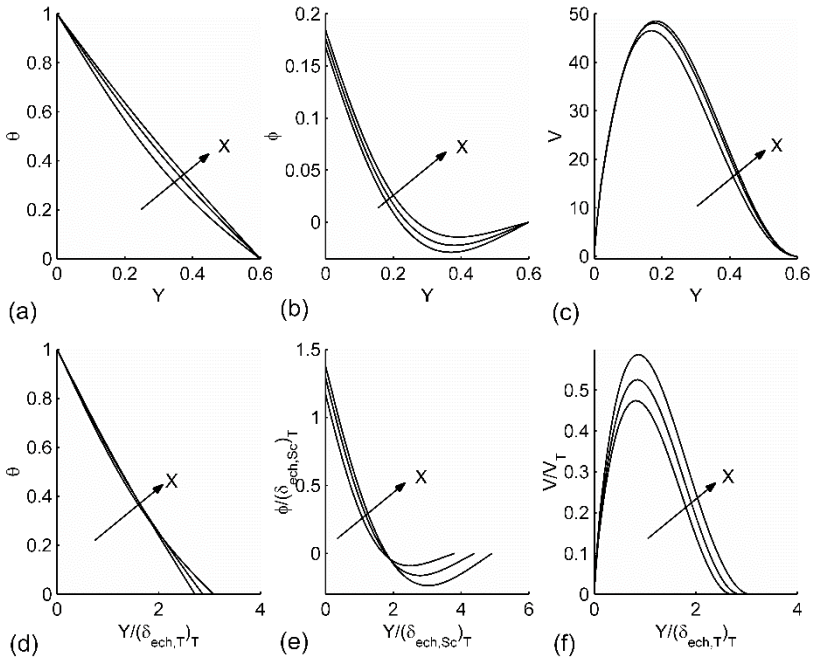

Fig. 5. The (a) θ, (b) φ and (c) V variations as a function of Y and the scaled (d) temperature, (e) concentration and (f) vertical velocity plots for the abscissa: 3, 4 and 5.

The parameters set: $Ra = 5000$, $N = 5$, $Le = 2$, $Pr = 0{,}72$, $S_C = 0.04$, is used to exemplify the $Ra \cdot S_C \cdot Sch^{4/3} / \left[Pr(1+Pr) \cdot N^3\right] < 1$ case.

Figure 2(b) indicates that we should encounter, at equilibrium, a heat driven convection regime (HDC_C) in the $X < X_{trz,C}$ region, a MDC_C regime in the $\left[X_{trz,C} - X_{S,C}\right]$ region and a MDC_{Sc} regime in the $X > X_{S,C}$ region. Equation (20) indicates $X_{trz,C} = 3.34$, while equation (30) indicates $X_{S,C} = 7.73$. A uniform grid of 61x451 points on a domain of 0.6x9.0 was used.

The results of the numerical modeling are presented by Figure 6. The θ (Figure 6(a)), φ/(1/N) (Figure 6(b)), Ψ (Figure 6(c)) and $\partial\varphi/\partial X$ (Figure 6(d)) contour plots reveal the following aspects: at the boundary, the concentration field exceeds $1/N = 1/5$ if $X > 1.6$, while $\partial\varphi/\partial X > 0.0$ at $X > 7.5$; these values are close to the scale analysis results. Each of the figures 7, 8 and 9 presents the plots and the scaled plots for three sections performed in the three regime regions emphasized above: HDC_C, MDC_C and MDC_{Sc}.

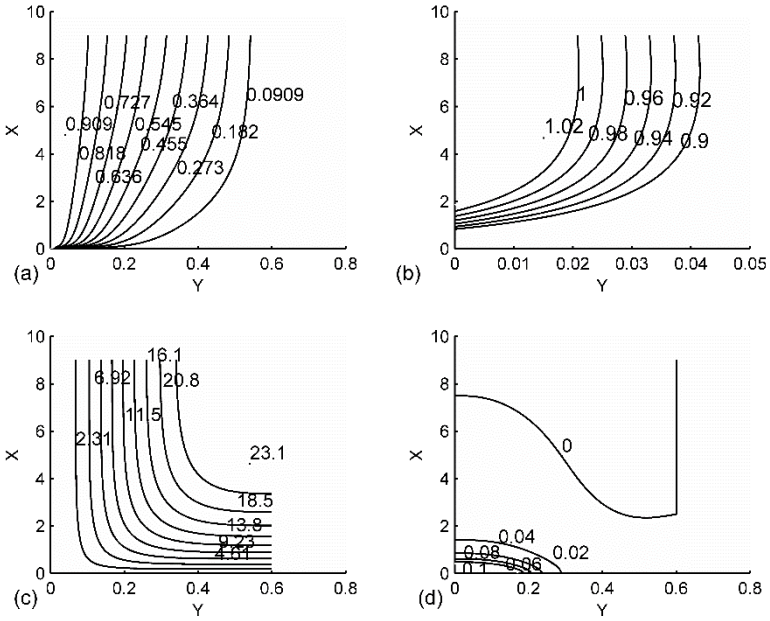

Fig. 6. The θ (a), φ/(1/N) (b), Ψ (c) and $\partial\varphi/\partial x$ (d) fields for $Ra = 5000$, $N = 5$, $Le = 1$, $Pr = 0.72$ and $S_C = 0.04$.

Figure 7(a), Figure 7(b) and Figure 7(c) presents the temperature, concentration and the vertical velocity plots for the abscissa: 0.5, 1.0 and 1.5, while Figure 7(d), Figure 7(e) and Figure 7(f) presents their scaled plots using the equations (16), (17) and (19).

Figure 8(a), Figure 8(b) and Figure 8(c) presents the temperature, concentration and the vertical velocity plots in the sections made at the abscissa: 4.0, 5.0 and 6.0, while Figures 8(d), (e) and (f) shows their scaled plots realised using the equation (33), (34), (35).

Similarly, Figures 9(a), (b) and (c) shows the temperature, concentration and vertical

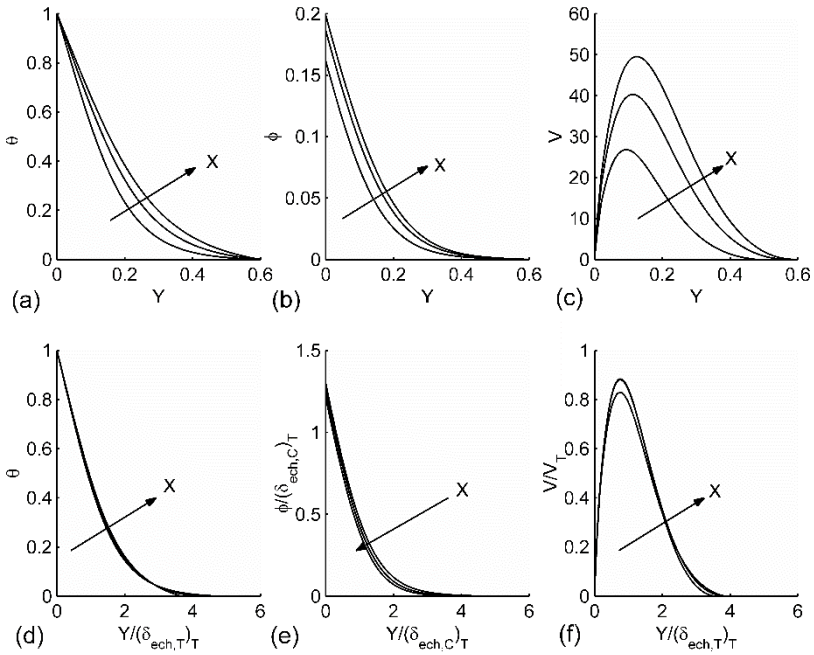

Fig. 7. The (a) θ, (b) φ and (c) V variations as a function of Y and the scaled (d) temperature, (e) concentration and (f) vertical velocity plots for the abscissa: 05, 1.0 and 1.5.

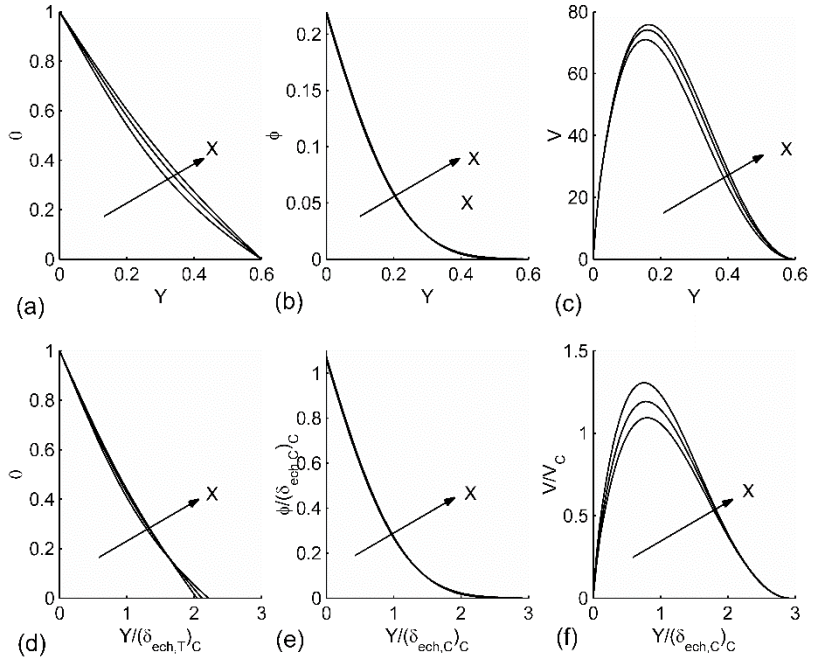

Fig. 8. The (a) θ, (b) φ and (c) V variations as a function of Y and the scaled (d) temperature, (e) concentration and (f) vertical velocity plots for the abscissa: 4.0, 5.0 and 6.0.

velocity plots for two abscissa: 8.0 and 9.0. Figure 9(d), Figure 9(e) and Figure 9(f) shows their scaled plots realised using the equations (28), (29) ad (31).

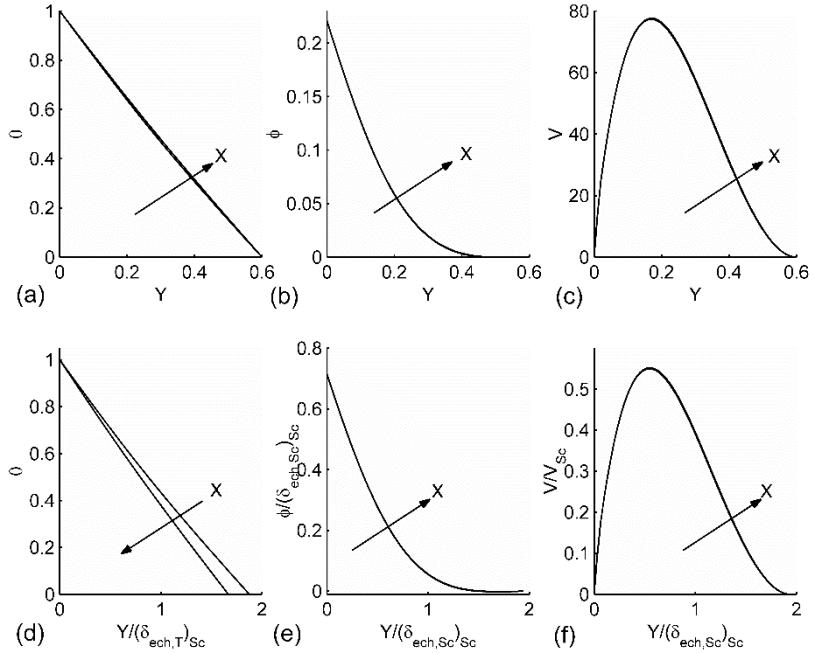

Fig. 9. The (a) θ, (b) φ and (c) V variations as a function of Y and the scaled (d) temperature, (e) concentration and (f) vertical velocity plots for the abscissa: 8.0 and 9.0.

The collapse of the scaled plots of Figures 7, 8 and 9 proves the validity of the scaled analysis results for the $\mathrm{Ra}\cdot S_C\cdot \mathrm{Sch}^2/\left|\mathrm{N}^3\,\mathrm{Pr}(1+\mathrm{Pr})\right|<1$ case.

6. Conclusions

The natural convection process developed in the boundary layer of a vertical plane wall continues to be the subject of new discoveries. If the temperature and the heat flux of a certain constituent are constant at the wall, then a constant temperature and a linearly mass stratified environment ($\mathrm{Pr}<1$, $\mathrm{Le}\geq 1$, $\mathrm{Sch}<1$) imposes special features on the natural convection process. Depending on the process parameters, we can encounter:

a heat driven convection regime along the wall if $\mathrm{Ra}\cdot S_C\cdot \mathrm{Sch}^2/\left|\mathrm{N}^3\,\mathrm{Pr}(1+\mathrm{Pr})\right|\geq 1$;

a succession of heat and mass driven convection regimes if

$\mathrm{Ra}\cdot \mathrm{S_C}\cdot \mathrm{Sch}^2 / \left[\mathrm{N}^3 \mathrm{Pr}(1+\mathrm{Pr})\right] < 1$.

This result is similar to the results found by previous scientific works:

for $\mathrm{Pr} < 1$, $\mathrm{Le} \geq 1$, $\mathrm{Sch} \geq 1$ case the coefficient that separates the two possibilities (HDC and HDC-MDC) is $\mathrm{Ra}\cdot \mathrm{S_C}\cdot \mathrm{Sch}^{4/3} / \left[\mathrm{N}^3 \mathrm{Pr}(1+\mathrm{Pr})\right]$, (Neagu, 2021);

for $\mathrm{Pr} \geq 1$, $\mathrm{Le} \geq 1$ case, the coefficient is $\mathrm{Ra}\cdot \gamma^2 \cdot \mathrm{S_C}\cdot \mathrm{Le}^{4/3} / \mathrm{N}^3$, where $\gamma = 1 - \left(1+\mathrm{Pr}^{1/2}\right)^{-1}$, (Neagu, 2018).

These results open the gate for further scientific paths:

a closer analysis of the way in which the non-dimensionalisation process is realised for these particular cases.

a closer analysis of the implications that these results could have on the stability management of the natural convection process.

References

[1] Armfield, S. W., Patterson, J. C. and Lin, W. (2007). Scaling investigation of the natural convection boundary layer on an evenly heated plate, International Journal of Heat and Mass Transfer, 50, 1592-1602

[2] Bejan, A. (1995). Convection Heat Transfer (2nd ed.). New York, U.S.A.: John Wiley & Sons

[3] Lin, W, Armfield, S. W., Patterson, J. C. (2008). Unsteady natural convection boundary layer flow of a linearly-stratified fluid with Pr<1 on an evenly heated semi-infinite vertical plate, International Journal of Heat and Mass Transfer, 51, 327–343

[4] Mongruel, A., Cloitre, M. and Allain, C. (1996). Scaling of boundary-layer flows driven by double-diffusive convection, International Journal of Heat and Mass Transfer, 39, 3899-3910

[5] Neagu, M. (2018). Natural convection near a vertical wall of constant mass flux and temperature situated in a mass stratified fluid, IOP Conference Series: Materials Science and Engineering 444 0822020, 1–14, doi: 10.1088/1757-899X/444/8/0822020

[6] Neagu, M. (2021). Heat/mass driven natural convection of air near a boundary of constant mass flux and temperature, Journal of Multidisciplinary Engineeering Science and Technology, 8(11), 14727-14735, Retrieved from http://www.jmest.org/vol-8-issue-11-november-2021/

[7] Patterson, J. C., Lei, C., Armfield, S. W. and Lin, W. (2009). Scaling of unsteady natural convection boundary layers with a non-instantaneous initiation, International Journal of Thermal Sciences, 48, 1843-1852

[8] Saha, S. C., Patterson, J. C. and Lei, C. (2010). Natural convection boundary–layer adjacent to an inclined flat plate subject to sudden and ramp heating, International Journal of Thermal Sciences, 49, 1600-1612

[9] Saha, S. C., Brown, R. J. and Gu, Y. T. (2012). Scaling of the Prandtl number of the natural convection boundary layer of an inclined flat plate under uniform surface heat flux, International Journal of Heat and Mass Transfer, 55, 2394-2401

[10] Tannehill, J. C., Anderson, D. A. & Pletcher, R. H. (1997). Computational Fluid Mechanics and Heat Transfer (2nd ed.). Washington, U.S.A.: Taylor&Francis

Appendix

Nomenclature

C dimensional concentration of the dissolved species
D diffusion coefficient of the species
g gravitational acceleration
k thermal conductivity of the fluid
h height of the computational domain
H dimensionless height of the computational domain
HDC heat driven convection regime
L characteristic length
Le Lewis number, (α/D)
m_w constant mass flux at the wall
MDC mass driven convection regime
N buoyancy ratio, $[\beta_c(m_w L/D)]/[\beta_t(T_w - T_{\infty,0})]$
p the environment pressure
Pr Prandtl number, ν/α
Ra Rayleigh number, $[g\beta_t(T_w - T_{\infty,0})L^3/\alpha\nu]$
s_C environment mass stratification parameter, $(dC_{\infty,x}/dx)$
S_C non-dimensional mass stratification parameter, $[s_C/(m_w L/D)]$
Sch Smith number, ν/D
t dimensional time
t_s time when the $v\cdot\partial C/\partial x$ term becomes dominant in the left hand side of Eq. (5)
t_{trz} dimensional time when the transition to a mass driven convection regime takes place
T dimensional temperature
T_w constant temperature at the wall
u,v dimensional velocity components
U,V dimensionless velocity components, uL/α, vL/α
x,y dimensional Cartesian coordinates
X,Y non-dimensional Cartesian coordinates, x/L, y/L
$(\ )_C$ value defined in a mass driven convection regime where $\partial C/\partial x \geq s_C$

$( )_{Sc}$ value defined in a mass driven convection regime where $\partial C/\partial x < s_C$

$( )_T$ value defined in a heat driven convection regime

Greek symbols

α thermal diffusivity

β_T the coefficients of volumetric expansion with temperature, $(-1/\rho)(\partial\rho/\partial T)_P$

β_C the coefficients of volumetric expansion with concentration, $(-1/\rho)(\partial\rho/\partial C)_P$

Γ_w dimensional concentration gradient at the wall, (m_w/D)

δ boundary-layer thickness

δ_C boundary-layer thickness of the concentration field

φ non-dimensional concentration of the dissolved species, $[(C-C_{\infty,x})/(m_w L/D)]$

ν kinematic viscosity

θ non-dimensional temperature, $[(T-T_\infty)/(T_w-T_\infty)]$

ρ fluid density

τ non-dimensional time, $\tau = t\alpha/L^2$

ψ dimensional stream function

Ψ non-dimensional stream function, ψ/α

ζ dimensionless vorticity

Subscripts

0 reference value

∞ condition at infinity

T related to the temperature field

ech equilibrium state

Sc the $V\cdot S_C$ term is dominant in the left side of Eq. (5)

C the $V\cdot\partial\varphi/\partial X$ term is dominant in the left hand side of Eq. (5)

v Related to the velocity field

x evaluated at abscissa x